

Disulfonamide Piperazine Derivatives: Synthesis, Characterization, Crystal Structures Studies, and Evaluation of Cell Proliferation Activity

L. Beliyah^a, A. Dilkalal^b, Vinaya^a, U. Basavaiah^c, S. Parkin^d, R. J. Butcher^e,
H. S. Yathirajan^a, and Y. B. Basavaraju^{a,*}

^a Department of Studies in Chemistry, University of Mysore, Mysore, 570006 India

^b Department of Botany, Bangalore University, Bangalore, 560056 India

^c JSS Arts, Science and Commerce College, Belagavi, 591307 India

^d Department of Chemistry, University of Kentucky, Lexington, 40506 USA

^e Department of Chemistry, Howard University, Washington, 20059 USA

*e-mail: ybb2706@gmail.com

Received December 18, 2023; revised April 13, 2024; accepted April 14, 2024

Abstract—In the present study, disulfonamides piperazine derivatives were synthesized by Hinsberg reaction of various sulfonyl chlorides with 2-(piperazin-1-yl)ethanamine and evaluation their cell proliferation activity. All the synthesized compounds were characterized by ¹H, ¹³C NMR, mass spectrometry and X-ray crystallographic techniques. X-ray diffraction studies revealed that the central piperazine ring and two terminal substituted sulfonyl phenyl rings joined by sulfonamide linkage are present in every structure. The cell proliferation activity of synthesized compounds was measured on human buccal mucosa oral fibroblast primary cell lines. Among the synthesized compounds, 4-nitro-*N*-(2-{4-[(4-nitrophenyl)sulfonyl]piperazin-1-yl}ethyl)benzenesulfonamide, 4-(trifluoromethyl)-*N*-[2-(4-[4-(trifluoromethyl)phenyl]sulfonyl]piperazin-1-yl)ethyl]benzenesulfonamide and 2-nitro-*N*-(2-{4-[(2-nitrophenyl)sulfonyl]piperazin-1-yl}ethyl)benzenesulfonamide showed potential activity against tested cell lines.

Keywords: piperazine disulfonamides, cell proliferation assay, X-ray crystallography

DOI: 10.1134/S1070363224080267

INTRODUCTION

Wounds are a major global health issue with serious commercial and social ramifications for hospitals, patients, and carers [1]. Physical, thermal, or chemical injuries can create an opening or crack in the skin's integrity or alter the anatomical integrity of living tissues [2]. Inflammation, proliferation, extracellular matrix formation, and finally remodeling are the stages of wound healing [3]. During the proliferative phase, fibroblasts spread and secrete many growth factors, including vascular endothelial growth factor (VEGF) and type I collagen [4]. The field of science is actively exploring inventive methods and approaches to create materials that aid the regeneration and healing of wounds [5, 6]. Sulfonamides, a significant class of drugs, displays a wide range of biological activities, such as anticancer

[7], anti-inflammatory [8] antibacterial [9–13], antifungal [14], antiprotozoal [15], antiviral [16], antimalarial [17], antitumor [18–20], carbonic anhydrase inhibitors [21–24], antidiabetic [25], anticonvulsant [26], anti-obesity [27], antidiuretic [28, 29], hypoglycaemic [30], antineuropathic pain [31], matrix metalloproteinase and bacterial protease. The presences of a heterocyclic ring in sulfonamides enhances its biological activities. Piperazine sulfonamides are important pharmacophore that can be found in bioactive compounds used in a number of different therapeutic areas. It has been revealed that piperazines carrying benzene sulfonyl groups showed anticancer [32], anti-allergic [33], neuronal nicotinic acetylcholine receptors [34], antibacterial, antiacetylcholinesterase [35] and selective covalent inhibitors of transglutaminase 2 for Huntington's disease [36]. However, the ethylene group between nitrogen and nitrogen provide the most

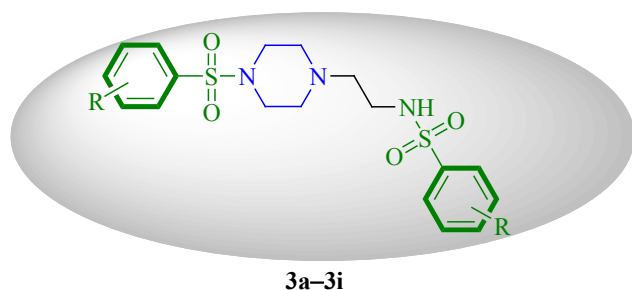


Fig. 1. General structure of disulfonamide-containing piperazine derivatives **3a–3i**.

active compounds. The activity of sulfonyl piperazines can be enhanced by inserting a β -aminoethyl group between the sulfonyl group and the piperazine nucleus [37]. Fibroblasts are group of connective tissue that plays an important role in wound healing, and also in tumor progression and metastasis [38]. The proliferative rate of oral mucosal fibroblast cells is high which regards to its quick wound healing activity [39].

The literature review suggests that so far there are no reports on crystal structure and proliferative studies of disulfonamide-containing piperazine derivatives. In view of the above finding and importance of piperazine and sulfonamides, in continuation of our research interest on bioactive organic compounds, in the current study sought to synthesise certain disulfonamide-containing piperazine derivatives **3a–3i** by NH-coupling reaction with various sulfonyl chlorides (Fig. 1, Scheme 1) and investigate their proliferative or wound healing activity on Oral buccal mucosa fibroblast primary cell lines.

RESULTS AND DISCUSSION

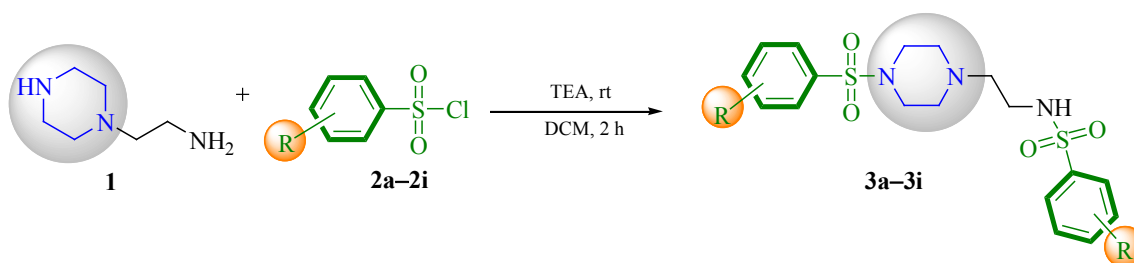
Disulfonamide-containing piperazine derivatives were synthesized by using available method [37]. Briefly,

piperazine **1** reacted with aromatic sulfonyl chlorides **2a–2i** in the presence of triethyl amine (TEA) as a base in dichloromethane at room temperature to afford the title of disulfonamide-containing piperazine derivatives **3a–3i** (Scheme 1). Synthesized derivatives furnished in moderate to high yields and melting point are reported in Table 1. The structures of the compounds were elucidated by ^1H , ^{13}C NMR, mass spectrometry and single crystal X-ray crystallographic studies (see Supplementary Information).

X-Ray crystallography studies. X-Ray crystallography diffraction data for all crystals were collected on a Bruker D8 Venture dual source diffractometer at 90 K (or 180 K for **3i** due to a destructive phase transition) using φ and ω scans. All structures were solved using SHELXT [40–41] and refined using SHELXL-2019/2 [42, 43]. The structures of **3a**, **3b**, **3d–3g**, and **3i** were also determined by X-ray diffraction. In all structures, one of the sulfonamide groups has an intermediate ethyl chain between it and the piperazine ring while the other is attached directly to the N in the piperazine ring. The structure of **3i** had whole molecule disorder and was refined using equivalent metrical parameters and the SAME command in SHELXL-2019/2 with occupancies of 0.907(2) and 0.093(2) respectively. The structure of **3g** was twinned by reticular pseudomerohedry [44]. X-Ray crystallographic data, molecular structure, packing diagram and crystal explorer fingerprint plots for compounds **3a**, **3b**, **3d**, and **3e** are presented in Table 2 and Figs. 2–13. Data for other compounds (**3f–3i**) are shown in Supplementary Information.

Crystal structural analysis of the Cambridge Structural Database [45] shows that no similar molecules have been structurally characterized. For these structures, except for **3e** which is a hydrochloride salt, only one of the sulfonamide moieties contains an N–H group since

Scheme 1.



R = 4-CH₃ (**a**), 4-NO₂ (**b**), 4-CF₃ (**c**), 2-NO₂ (**d**), H (**e**), 4-F (**f**), 4-Cl (**g**), 2-thienyl (**h**), 4-OCH₃ (**i**).

Table 1. Chemical structure, yields and melting points of synthesized compounds **3a–3i**

Compound	Sulfonyl moiety	Molecular formula	Molecular weight	mp, °C	Yield, %
3a		C ₂₀ H ₂₇ O ₄ N ₃ S ₂	438.192	165–168	94
3b		C ₁₈ H ₂₁ O ₈ N ₅ S ₂	500.018	158–161	97
3c		C ₂₀ H ₂₁ O ₄ F ₆ N ₃ S ₂	546.567	178–180	84
3d		C ₁₈ H ₂₁ O ₈ N ₅ S ₂	500.01	133–135	98
3e		C ₁₈ H ₂₃ O ₄ N ₃ S ₂	410.116	148–150	89
3f		C ₁₈ H ₂₁ O ₄ F ₂ N ₃ S ₂	446.094	137–139	91
3g		C ₁₈ H ₂₁ O ₄ Cl ₂ N ₃ S ₂	478.033	164–167	95
3h		C ₁₄ H ₂₁ O ₄ N ₃ S ₄	422.98	181–183	85
3i		C ₂₀ H ₂₇ O ₆ N ₃ S ₂	470.35	124–126	84

the other is directly attached to the N of the piperazine ring. Since these are all biologically active molecules their molecular shapes are an important aspect of their activity. These shapes are influenced by both intra- and intermolecular interactions such as hydrogen bonding

and other weaker forces such as C–H···O and C–H···N interactions. Thus, in a discussion of each structure this will be highlighted.

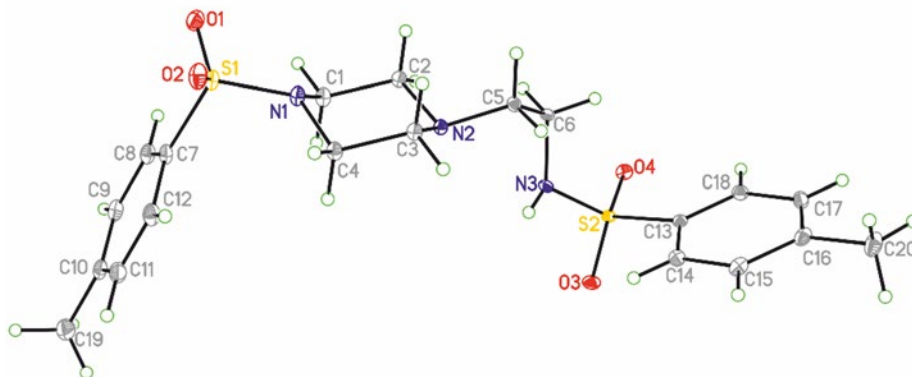
Compound **3a** crystallizes in the monoclinic space group $P2_1/c$ with one molecule in the asymmetric unit.

Table 2. Crystallographic data for compounds **3a**, **3b**, **3d**, and **3e**

Parameter	3a	3b	3d	3e
Chemical formula	C ₂₀ H ₂₇ N ₃ O ₄ S ₂	C ₁₈ H ₂₁ N ₅ O ₈ S ₂	C ₁₈ H ₂₁ N ₅ O ₈ S ₂	C ₁₈ H ₂₄ N ₃ O ₄ S ₂ ·Cl·H ₂ O
<i>M_r</i>	437.56	499.52	499.52	463.99
Crystal system Space group	Monoclinic	Monoclinic	Monoclinic	Triclinic
Space group	<i>P</i> 2 ₁ / <i>c</i>	<i>P</i> 2 ₁ / <i>n</i>	<i>P</i> 2 ₁ / <i>c</i>	<i>P</i> -1
Temperature, K	90	90	90	90
<i>a</i> , Å	19.6233(6)	13.5810(3)	12.4906(4)	6.0720(2)
<i>b</i> , Å	6.0845(2)	8.1360(2)	15.0070(3)	11.5700(3)
<i>c</i> , Å	17.5311(5)	19.9031(5)	12.4637(4)	15.1171(5)
α , deg	90	90	90	85.161(1)
β , deg	90.292(1)	94.936(1)	116.676(1)	83.304(1)
γ , deg	90	90	90	84.288(1)
<i>V</i> , Å ³	2093.15(11)	2191.04(9)	2087.6(1)	1046.69(6)
<i>Z</i>	4	4	4	2
Radiation type	MoK α	MoK α	MoK α	MoK α
μ , mm ⁻¹	0.29	0.30	0.32	0.42
Crystal size, mm	0.32×0.24×0.04	0.28×0.22×0.07	0.24×0.22×0.17	0.38×0.37×0.20
<i>T_{min}</i> , <i>T_{max}</i>	0.847, 0.959	0.849, 0.971	0.911, 0.971	0.907, 0.971
Number of measured, independent and observed [<i>I</i> > 2 σ (<i>I</i>)] reflections	31829, 4791, 4313	39735, 5030, 4425	33041, 4783, 4312	37968, 4783, 4311
<i>R_{int}</i>	0.034	0.036	0.040	0.038
<i>R</i> [<i>F</i> ² > 2 σ (<i>F</i> ²)], <i>wR</i> (<i>F</i> ²), <i>S</i>	0.033, 0.086, 1.07	0.034, 0.087, 1.05	0.030, 0.077, 1.03	0.028, 0.069, 1.04
Number of reflections	4791	5030	4783	4783
Number of parameters	268	302	303	278
Number of restraints	0	0	0	0
$\Delta\rho_{\max}/\Delta\rho_{\min}$, e/Å ³	0.46/−0.42	0.44/−0.45	0.41/−0.44	0.39/−0.41

It consists of two terminal toluene rings linked to a central piperazine ring via sulfonamide groups (Fig. 2). Interestingly, the piperazine ring is almost perpendicular to its adjacent toluene ring, with a torsion angle of

66.38(6)°. In the packing of **3a**, both sulfonamide groups participate in chains of weak C–H···O interactions propagating in the *b*-direction. This is likely the cause of the above conformation of the piperazine ring and its

**Fig. 2.** General view of the molecule of compound **3a** in the crystal. Atomic displacement parameters are at the 30% probability level.

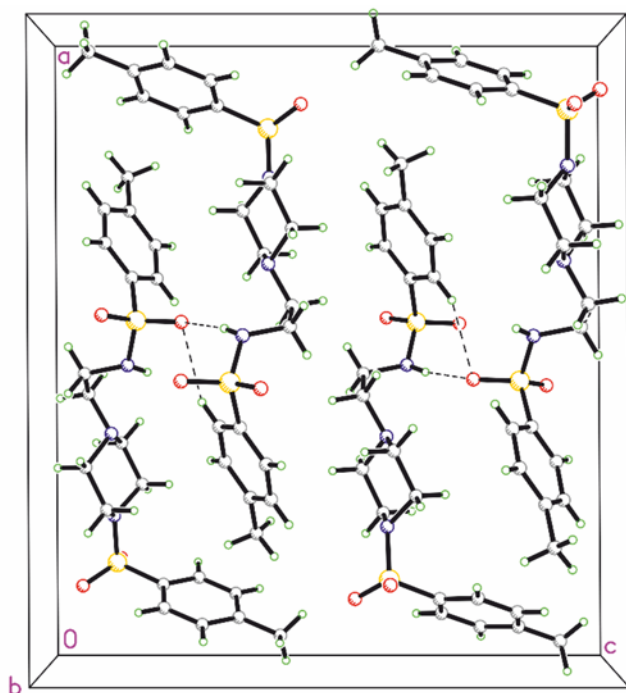


Fig. 3. Crystal packing diagram for **3a** viewed along the *b* axis. N–H···O and C–H···O interactions are shown by dashed lines.

adjacent toluene ring. Additionally, there is an $R_3^3(12)$ [41] ring of weak C–H···O and N–H···O hydrogen interactions between three adjacent molecules (symmetry codes: $x, 1+y, z; 1-x, 1/2+y, 3/2-z$). These are shown in the packing diagram (Fig. 3) and the C–H···O and N–H···O fingerprint plots (Fig. 4) determined by Crystal Explorer [44].

Compound **3b** crystallizes in the monoclinic space group $P2_1/n$ with one molecule in the asymmetric unit. Its structure is analogous to that of **3a**, except with terminal nitrophenyl rings instead of toluene rings (Fig. 5). The conformation of this molecule is a result of a combination of a number of C–H···O and N–H···O interactions. In this structure the piperazine ring is almost perpendicular to both its adjacent nitrophenyl ring and the other terminal ring, with torsion angles of $84.65(5)^\circ$ and $80.70(6)^\circ$ respectively. The former is likely due to the presence of a weak C–H···O interaction between an oxygen on the terminal nitrophenyl group and the piperazine ring in an adjacent molecule (symmetry code: $1-x, -y, 1-z$). Additionally, the sulfonamide group of an adjacent molecule's piperazine ring forms a $R_2^1(6)$ ring of weak C–H···O interactions with the piperazine ring, which further contributes to the above conformation of the two rings (symmetry code: $x, 1+y, z$; Fig. 6). A similar interaction is also likely the cause of the latter conformation. Finally, a chain of weak C–H···O interactions between the terminal nitrophenyl ring adjacent to the piperazine ring and the piperazine ring of an adjacent molecule propagating in the *b*-direction further contributes to the former conformation (symmetry code: $1-x, -y, 1-z$).

Another aspect of the packing involves close contacts between the nitro groups of one phenyl ring. The distance between O⁷ in one ring and N⁵ in the other is $2.9911(19)$ Å with symmetry code of $2-x, 1-y, 1-z$. These are summarized in the fingerprint plots of the N–H···O, C–H···O, and N···O interactions (Fig. 7).

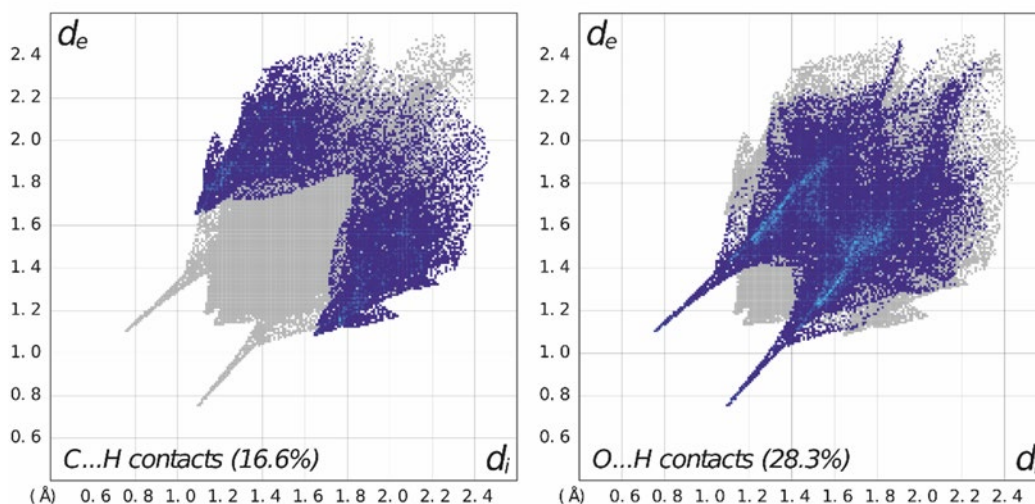


Fig. 4. Crystal explorer fingerprint plots for **3a** showing C–H···O and N–H···O interactions, respectively, as prominent spikes.

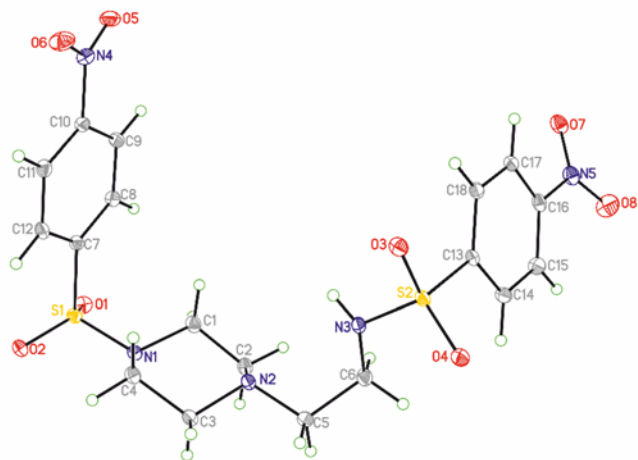


Fig. 5. General view of the molecule of compound **3b** in the crystal. Atomic displacement parameters are at the 30% probability level.

Compound **3d** crystallizes in the monoclinic space group $P2_1/c$ with one molecule in the asymmetric unit. Its structure is analogous to that of **3b**, except with nitro groups occupying an *ortho*-position with respect to the sulfonamide groups in both terminal nitrophenyl rings. This conformation allows for the formation of an intramolecular $N-H\cdots O$ hydrogen bond between a sulfonamide group and a nitro group on a terminal nitrophenyl moiety (Fig. 8). As a result, the nitro group is almost parallel to its ring, with a torsion angle of $26.30(5)^\circ$. In contrast, the other nitro group is almost perpendicular to its ring, with a torsion angle of $73.62(4)^\circ$. Similarly, to **3b**, the piperazine ring is again almost perpendicular to its adjacent nitrophenyl ring, with a torsion angle of $78.72(5)^\circ$. However, unlike the previous two structures, the other terminal nitrophenyl ring is almost parallel to the piperazine ring with a torsion angle of $40.56(16)^\circ$. This can likely be explained by the above hydrogen bond between the sulfonamide group and the *ortho*-nitro group.

Another aspect of the packing involves intermolecular close contacts between the nitro groups of one phenyl ring

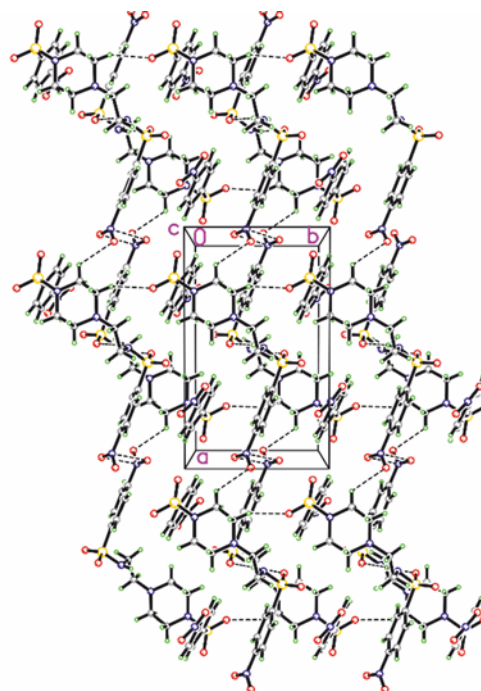


Fig. 6. Crystal packing diagram for **3b** viewed along the c axis showing $C-H\cdots O$ interactions (shown as dashed lines) between an oxygen on the terminal nitrophenyl group and the piperazine ring in an adjacent molecule (symmetry code: $1-x, -y, 1-z$).

and the nitro group of the other phenyl ring (Fig. 9). The distance between O^1 in one ring and N^5 in the other is $2.9893(19)$ Å (symmetry code: $1-x, 1-y, 1-z$). The nitro O^7 atom is also involved in another short contact to O^7 on an adjacent molecule [$O^7\cdots O^7$, $2.844(2)$; symmetry code: $-x, 1-y, 1-z$]. There are several additional weak $C-H\cdots O$ interactions ($C^5-H^5\cdots O^6$, symmetry code: $-x, 3/2+y, 1/2-z$; $C^9-H^9B\cdots O^6$, symmetry code: $-x, -1-y, -z$; $C^{11}-H^{11}B\cdots O^6$, symmetry code: $-x, -1-y, -z$; $C^{15}-H^{15}\cdots O^3$, symmetry code: $-x, -1-y, -z$; $1-z, 3/2+y, 3/2-z$; $C^{18}-H^{18}\cdots O^5$, symmetry code: $-x, -1-y, -z$; $-x, 3/2+y, 1/2-z$). These all contribute to the folding of the molecule. These $N-H\cdots O$, $C-H\cdots O$, $N\cdots O$, and $O\cdots O$ interactions are illustrated in their respective fingerprint plots (Fig. 10).

Compound **3e** crystallizes in the triclinic space group $P-1$ with one formula unit in the asymmetric unit. Here the stoichiometry is $[C_{18}H_{24}N_3O_4S_2]^+$, Cl^- , H_2O and thus the disulfonamide moiety is a cation along with a chloride anion and water of solvation. Its structure is analogous to that of **3a**, except with terminal phenyl rings instead of terminal toluene rings (Fig. 11). The nitrogen in the

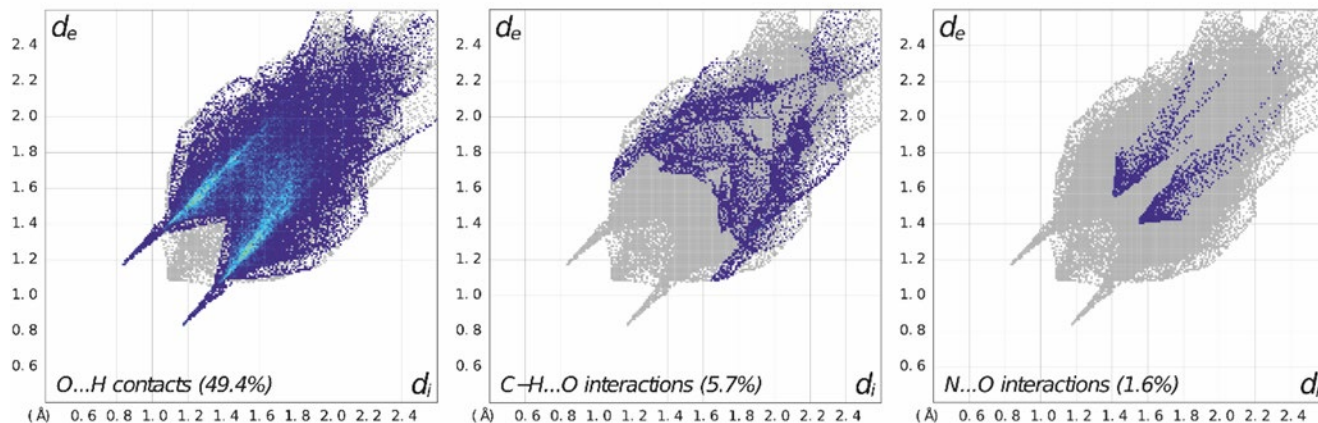


Fig. 7. Crystal Explorer fingerprint plots for **3b** showing N–H···O, C–H···O, and N···O interactions, respectively, as prominent spikes.

piperazine ring linked to the ethyl chain is protonated, making the overall structure a cation.

The disulfonamide cation, chloride cation and water molecule form an $R_2^2(9)$ ring of interactions with the two NH groups in the structure. Interestingly, this

conformation also allows one of the ethyl carbons to form a weak C–H···O interaction with its adjacent sulfonamide group. The piperazine ring and its adjacent phenyl ring are again almost perpendicular, with a torsion angle of $62.36(5)^\circ$, although they are less so than the previous two structures (Fig. 12). This is likely due to the presence of

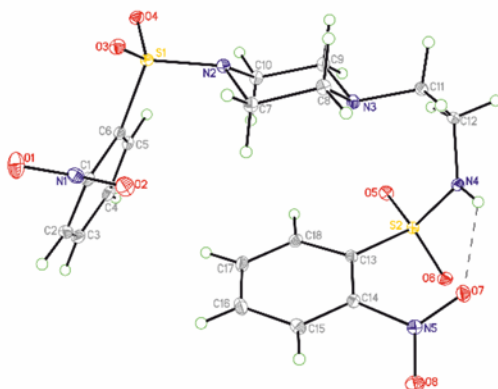


Fig. 8. General view of the molecule of compound **3d** in the crystal. Intramolecular N–H···O hydrogen bond between a disulfonamide group and a nitro group on a terminal nitrophenyl moiety are shown as dashed lines.

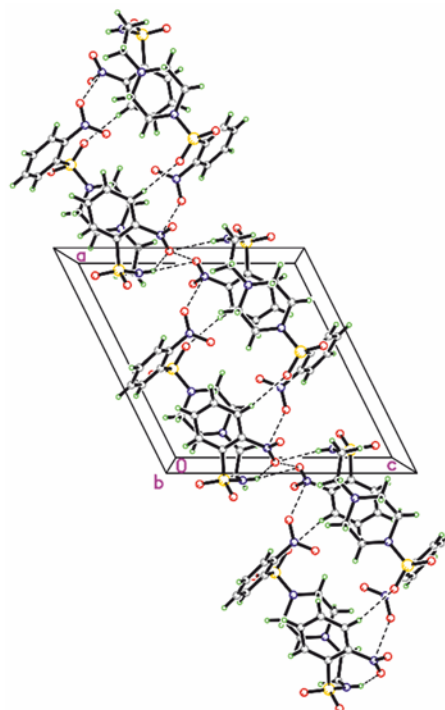


Fig. 9. Packing diagram for **3d** viewed along the c axis showing the intermolecular close contacts between the nitro groups of one phenyl ring and the nitro group of the other phenyl ring (shown as dashed lines; symmetry code: $1-x, 1-y, 1-z$).

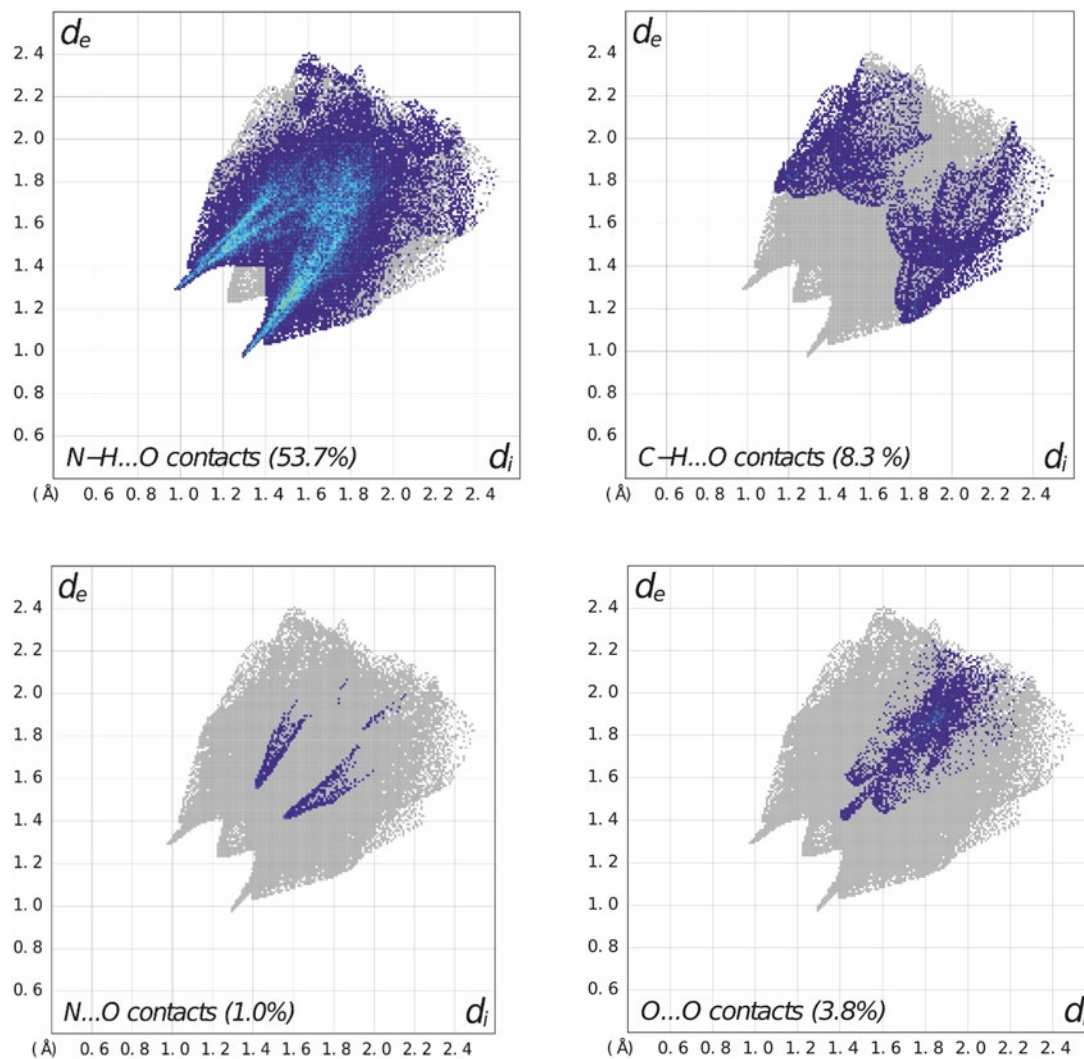


Fig. 10. Crystal Explorer fingerprint plots for **3d** showing N-H...O, C-H...O, N...O and O...O interactions, respectively, as prominent spikes.

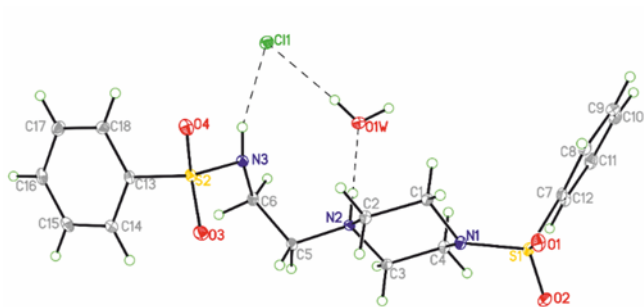


Fig. 11. General view of the molecule of compound **3e** in the crystal showing the cation, anion and water of solvation all linker by hydrogen bonds (shown as dashed lines). Atomic displacement parameters are at the 30% probability level.

an N-H...O hydrogen bond between the NH group in the piperazine ring and the solvent water molecule. This interaction, along with the weak C-H...O interaction and interactions made by the chloride anion, forms an R^4_3 (11) ring of interactions within the asymmetric unit itself. In the packing of **3e**, there is both an R^4_4 (16) ring of weak C-H...O interactions between the sulfonamide groups and piperazine rings of adjacent molecules (symmetry code: $-x, 2-y, 1-z$) and a R^2_2 (12) ring of weak C-H...O interactions between the same groups. The latter involves the sulfonamide group linked to the phenyl ring adjacent to the piperazine ring, while the former involves the sulfonamide group linked to the other phenyl ring. Additionally, the solvent water molecules and chloride

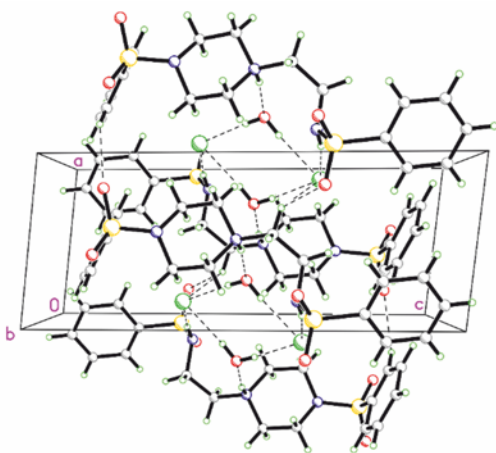


Fig. 12. Crystal packing diagram for **3e** viewed along the *b* axis showing the C–H...O, N–H...O, N–H...Cl and O–H...Cl interactions (shown as dashed lines).

anions of adjacent molecules form an $R^4_2(8)$ ring that can be seen propagating in the *a*-direction. Similarly, to **3a**, both sulfonamide groups form chains of weak C–H...O interactions with the phenyl rings of adjacent molecules propagating in the *a*-direction. These C–H...O, N–H...O, and combined N–H...Cl/O–H...Cl interactions are shown in fingerprint plots (Fig. 13).

Cell proliferation assay. The cell proliferation was evaluated using an MTT [3-(4,5-dimethylthiazol-2-yl)-2,5-diphenyltetrazolium bromide] is a tetrazolium reduction assay is a homogeneous cell viability test

established. Primarily this assay was developed as a non-radioactive substitute for using ^3H -thymidine incorporation into DNA to measure cell proliferation [46]. The cell proliferation is one of sequential phase in the wound healing process. In the present study the compounds **3a–3i** were treated with oral fibroblast with a dose dependent concentration ranging from 15.6 to 125 $\mu\text{g/mL}$. The cell viability percentage of compounds **3a–3i** displayed various degree of cell proliferative activity against the selected cell line, the cell proliferation percentage of the synthesized compounds shows a dose depended manner of cell proliferation with a maximum of 99.78 ± 0.65 at 125 $\mu\text{g/mL}$. Among the synthesized compounds **3b**, **3c** and **3d** showed potent proliferation of oral fibroblast at 125 $\mu\text{g/mL}$ against human buccal mucosa cell lines with a % cell viability of compare with control, this could be presence electron withdrawing groups (EWGs) *para*- CF_3 (**3c**) and *ortho*- NO_2 (**3d**). Whereas, compounds **3f** and **3g** also substituted with EWGs such as., fluoro and chloro at *para* position of sulfonyl phenyl ring, showed dominant activity but lesser than that of **3c** and **3d**. The electron donating groups (EDGs) of methyl and methoxy containing compounds (**3a** and **3i**) and other compounds (**3e** and **3h**) showed moderate to good cell proliferation activity at various concentrations. The percentage cell proliferation activity of synthesized compounds with human buccal mucosa oral fibroblast primary cell lines are showed in Fig. 14.

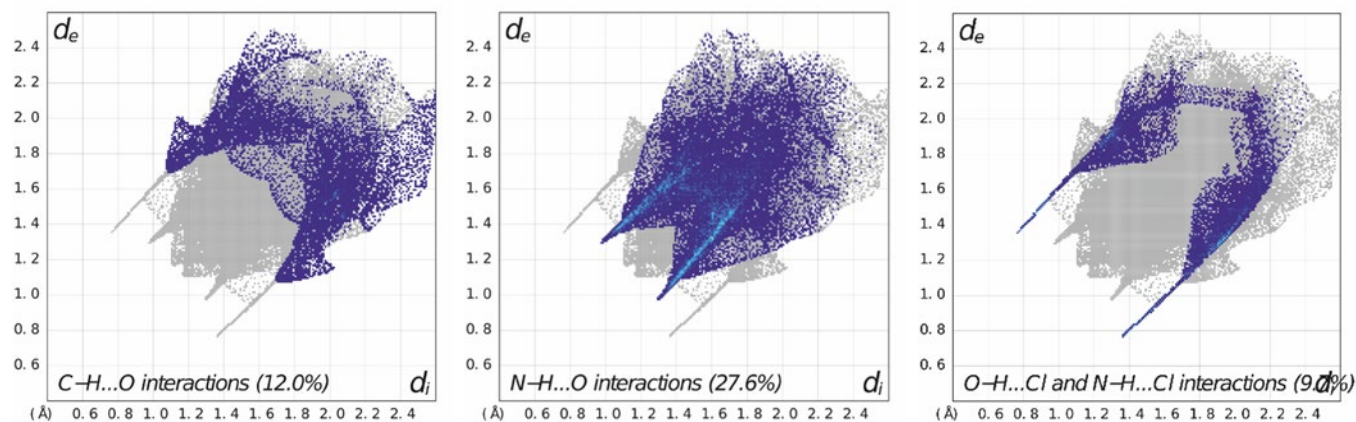


Fig. 13. Crystal explorer fingerprint plots for **3e** showing C–H...O, N–H...O, and combined N–H...Cl/O–H...Cl interactions, respectively, as prominent spikes.

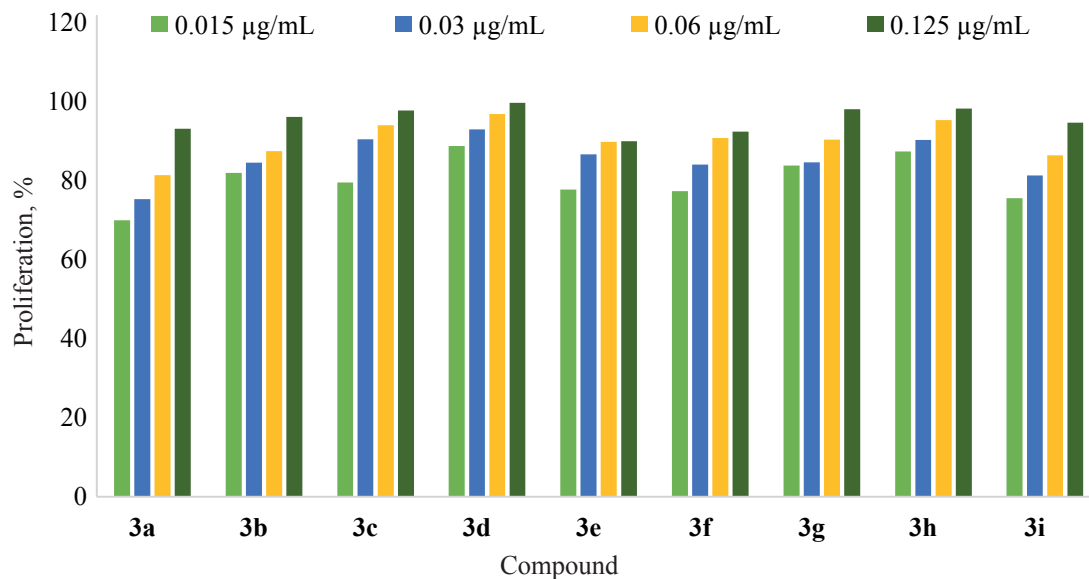


Fig. 14. Cell proliferation activity of synthesized compounds **3a–3i** against human buccal mucosa oral fibroblast primary cell lines.

CONCLUSIONS

In summary, we have successfully synthesized a disulfonamide piperazine derivatives **3a–3i** using an available synthetic procedure. The structures of compounds were characterized by ^1H , ^{13}C NMR, mass spectrometry and single crystal X-ray diffraction technique. X-Ray diffraction studies showed that their conformations differed significantly as a result of the differing substitution present on the terminal sulfonyl phenyl rings. Cell proliferative studies indicates that all the compounds showed certain degree of activity but EWGs substituents containing derivatives (**3b**, **3c** and **3d**) being more proliferative against tested human buccal mucosa oral fibroblast primary cell lines.

EXPERIMENTAL

All reagents were purchased from Sigma Chemicals (USA) and used without further purification. All melting points were taken in open capillaries and are uncorrected. The purity and mass of the synthesized compounds was checked by LCMS. ^1H and ^{13}C NMR spectra were recorded in $\text{DMSO}-d_6$ with tetramethyl silane (TMS) as the internal standard at 400 and 100 MHz on a Bruker DRTX-400 spectrophotometer. Merck silica gel (60 to 120 meshes) was used for analytical TLC and column chromatography, respectively. Diffraction data for all

crystals were collected on a Bruker D8 Venture dual source diffractometer at 90 K (or 180 K for **3i** due to a destructive phase transition) using φ and ω scans. All structures were solved using SHELXT and refined using SHELXL-2019/2.

General procedure for the synthesis of compounds

3a–3i. To a solution of 2-(piperazin-1-yl)ethanamine **1** (100 mmol) in dichloromethane (DCM) (5.0 mL) at 0°C was added a substituted sulfonyl chloride **2** (225 mmol). Next, 2 mL of triethyl amine was added while the temperature was maintained between 0 and -5°C . The reaction mixture was then stirred at room temperature. The reaction progress was monitored by TLC (eluent: *n*-hexane–EtOAc, 2:2). The reaction mixture was extracted with ethyl acetate. The combined organic layers were washed with 0.5 N HCl, water, and brine, dried over anhydrous Na_2SO_4 and concentrated under reduced pressure to get the crude product. Further all the synthesized compounds were purified column chromatography over silica gel (60–120 mesh) using hexane–EtOAc (9:1) as eluent.

4-Methyl-N-[2-(4-tosylpiperazin-1-yl)ethyl] benzenesulfonamide (3a). Yield 94%, mp $165\text{--}168^\circ\text{C}$. ^1H NMR spectrum ($\text{DMSO}-d_6$, 400 MHz), δ , ppm: 8.85 s (1H, NH, secondary amine), 8.25–8.30 m (2H, Ar-H), 7.93–7.80 m (4H, Ar-H), 7.39–7.510 m (2H, Ar-H), 3.15 d (2H, ethyl-H, *J* 12.0 Hz), 2.80 d (4H, ethyl-H,

J 12.0 Hz), 2.30 d (6H, ethyl, *J* 36.0 Hz), 2.30 s (3H, CH₃). ¹³C NMR spectrum (DMSO-*d*₆, 100 MHz), δ_C, ppm: 143.0, 137.5, 137.0, 129.5, 128.0, 55.4, 53.7, 48.8, 40.5, 21.5. Mass spectrum (LCMS), *m/z*: 438.1927 [*M*]⁺, 439.1919 [*M*]⁺². Found, %: C 55.24; H 5.98; N 10.23; S 14.21. C₂₀H₂₇N₃O₄S₂. Calculated, %: C 54.90; H 6.22; N 9.60; S, 14.65.

4-Nitro-*N*-(2-{4-[(4-nitrophenyl)sulfonyl]piperazin-1-yl}ethyl)benzenesulfonamide (3b). Yield 97%, mp 158–161°C. ¹H NMR spectrum (DMSO-*d*₆, 400 MHz), δ, ppm: 9.80 s (1H, NH), 8.40–8.42 m (2H, Ar-H), 8.26–8.28 m (2H, Ar-H), 7.93–7.96 m (4H, Ar-H), 3.02 d (2H, ethyl-H, *J* 6.8 Hz), 2.79–2.84 m (4H, piperazine-H), 2.26–2.31 m (6H, ethyl + piperazine-H). ¹³C NMR spectrum (DMSO-*d*₆, 100 MHz), δ_C, ppm: 150.6, 149.8, 147.1, 140.94, 129.6, 128.4, 125.24, 124.7, 56.6, 51.9, 46.2, 45.9. Mass spectrum (LCMS), *m/z*: 500 [*M*]⁺, 501 [*M*]⁺². Found, %: C 44.47; H 4.87; N 13.23; S 13.13. C₁₈H₂₁N₅O₈S₂. Calculated, %: C 43.28; H 4.24; N 14.02; S 12.84.

4-(Trifluoromethyl)-*N*-(2-{4-[(trifluoromethyl)phenyl]sulfonyl}piperazin-1-yl)ethyl)benzenesulfonamide (3c). Yield 84%, mp 178–180°C. ¹H NMR spectrum (DMSO-*d*₆, 400 MHz), δ, ppm: 9.53 s (1H, NH), 7.54–8.14 m (8H, Ar-H), 2.02–3.33 m (12H, ethyl + piperazine-H). ¹³C NMR spectrum (DMSO-*d*₆, 100 MHz), δ_C, ppm: 136.1, 132.3, 131.8, 131.3, 130.8, 130.2, 129.7, 125.7, 124.4, 123.5, 122.5, 55.9, 51.4, 40.6. Mass spectrum (LCMS), *m/z*: 546 [*M*]⁺, 547 [*M*]⁺². Found, %: C 43.76; H 4.14; F 21.46; N 7.98; S 12.27. C₂₀H₂₁F₆N₃O₄S₂. Calculated, %: C 44.04; H 3.88; F 20.90; N 7.70; S, 11.75.

2-Nitro-*N*-(2-{4-[(2-nitrophenyl)sulfonyl]piperazin-1-yl}ethyl)benzenesulfonamide (3d). Yield 98%, mp 133–135°C. ¹H NMR spectrum (DMSO-*d*₆, 400 MHz), δ, ppm: 7.87–7.98 m (6H, Ar-H), 7.70–7.78 m (2H, Ar-H), 2.92–3.02 m (6H, ethyl), 2.31–2.46 m (6H, ethyl + piperazine-H). ¹³C NMR spectrum (DMSO-*d*₆, 100 MHz), δ_C, ppm: 148.5, 147.9, 135.6, 134.17, 133.9, 133.0, 132.7, 131.08, 129.9, 124.7, 56.57, 51.86, 45.87, 46.62. Mass spectrum (LCMS), *m/z*: 500 [*M*]⁺, 501 [*M*]⁺². Found, %: C 44.47; H 4.87; N 13.23; S 13.13. C₁₈H₂₁N₅O₈S₂. Calculated, %: C 43.28; H 4.24; N 14.02; S 12.84.

***N*-(2-[4-(Phenylsulfonyl)piperazin-1-yl]ethyl)benzenesulfonamide (3e).** Yield 89%, mp 148–150°C. ¹H NMR spectrum (DMSO-*d*₆, 400 MHz), δ, ppm: 10.80 s (1H, NH), 7.55–7.98 m (10H, Ar-H), 2.46–3.67 m (12H,

ethyl + piperazine-H). ¹³C NMR spectrum (DMSO-*d*₆, 100 MHz), δ_C, ppm: 134.2, 133.2, 130.1, 129.8, 127.07, 51.01, 45.8, 40.1. Mass spectrum (LCMS), *m/z*: 410 [*M*]⁺, 411 [*M*]⁺². Found, %: C 53.18; H 5.87; N 9.93; S 15.89. C₁₈H₂₃N₃O₄S₂. Calculated, %: C 52.79; H 5.66; N 10.26; S 15.66.

4-Fluoro-*N*-(2-{4-[(4-fluorophenyl)sulfonyl]piperazin-1-yl}ethyl)benzenesulfonamide (3f). Yield 91%, mp 137–139°C. ¹H NMR spectrum (DMSO-*d*₆, 400 MHz), δ, ppm: 9.30 s (1H, NH), 7.55–7.98 m (8H, Ar-H), 2.45–3.66 m (12H, ethyl + piperazine-H). ¹³C NMR spectrum (DMSO-*d*₆, 100 MHz), δ_C, ppm: 165.6, 140.0, 135.2, 130.7, 55.2, 53.5, 48.5, 40.5. Mass spectrum (LCMS), *m/z*: 446 [*M*]⁺, 447 [*M*]⁺². Found, %: C 49.02; H 4.87; F 9.14; N 10.03; S 14.87. C₁₈H₂₁F₂N₃O₄S₂. Calculated, %: C 48.53; H 4.75; F 8.53; N 9.43; S 14.39.

4-Chloro-*N*-(2-{4-[(4-chlorophenyl)sulfonyl]piperazin-1-yl}ethyl)benzenesulfonamide (3g). Yield 95%, mp 164–167°C. ¹H NMR spectrum (DMSO-*d*₆, 400 MHz), δ, ppm: 7.71–7.74 m (4H, Ar-H), 7.35–7.59 m (4H, Ar-H), 2.85–3.12 m (12H, ethyl + piperazine-H). ¹³C NMR spectrum (DMSO-*d*₆, 100 MHz), δ_C, ppm: 139.0, 137.7, 133.8, 130.2, 130.1, 129.8, 128.9, 51.5, 45.8, 40.02. Mass spectrum (LCMS), *m/z*: 478 [*M*]⁺, 479 [*M*]⁺². Found, %: C 44.87; H 4.17; Cl 15.05; N 9.15; S 13.14. C₁₈H₂₁Cl₂N₃O₄S₂. Calculated, %: C 45.19; H 4.42; Cl 14.82; N 8.78; S 13.40.

***N*-(2-[4-(Thiophen-2-ylsulfonyl)piperazin-1-yl]ethyl)thiophene-2-sulfonamide (3h).** Yield 85%, mp 181–183°C. ¹H NMR spectrum (DMSO-*d*₆, 400 MHz), δ, ppm: 10.94 s (1H, NH), 7.91–8.09 m (2H, Ar-H), 7.61–7.61 m (2H, Ar-H), 7.15–7.31 m (2H, Ar-H), 2.46–3.13 m (2H, ethyl + piperazine-H). ¹³C NMR spectrum (DMSO-*d*₆, 100 MHz), δ_C, ppm: 135.3, 134.4, 134.1, 133.4, 132.5, 129.15, 128.4, 55.23, 50.85, 43.86, 40.0. Mass spectrum (LCMS), *m/z*: 422 [*M*]⁺, 424 [*M*]⁺². Found, %: C 40.15; H 4.89; N 10.36; S 31.27. C₁₄H₁₉N₃O₄S₄. Calculated, %: C 39.89; H 4.54; N 9.97; S 30.42.

4-Methoxy-*N*-(2-{4-[(4-methoxyphenyl)sulfonyl]piperazin-1-yl}ethyl)benzenesulfonamide (3i). Yield 84%, mp 124–126°C. ¹H NMR spectrum (DMSO-*d*₆, 400 MHz), δ, ppm: 10.28 s (1H, NH), 7.67 m (4H, Ar-H), 7.05–7.16 m (4H, Ar-H), 3.81 br. s (6H, OCH₃), 2.29–3.11 m (12H, ethyl + piperazine-H). ¹³C NMR spectrum (DMSO-*d*₆, 100 MHz), δ_C, ppm: 163.5, 162.76, 130.4, 129.2, 127.4, 115.1, 114.7, 113.2, 56.3, 55.6, 51.1, 40.62. Mass spectrum (LCMS), *m/z*: 470 [*M*]⁺,

471 [M]⁺¹. Found, %: C 49.67; H 6.16; N 9.26; S 13.14. C₂₀H₂₇N₃O₆S₂. Calculated, %: C 51.16; H 5.80; N 8.95; S 13.66.

Procedure of cell proliferation assay. The cell proliferation was evaluated using an MTT [3-(4,5-dimethylthiazol-2-yl)-2,5-diphenyltetrazolium bromide] assay. Oral buccal mucosa fibroblast primary cells were seeded in a 96-well polystyrene culture plate at a density of 1×10⁴ cells per well and incubated overnight at 37°C in a 5% CO₂ incubator with 85% humidity. DMEM containing high glucose, 10% FBS and 1% penicillin/streptomycin was used as media. Next morning, cells were treated with various concentrations (15.6, 31.25, 62.5, 125 µg/mL) of compounds **3a–3i** and incubated for 24 h. The media were discarded and 100 µL of MTT working solution (0.5mg/mL) prepared in DMEM (without FBS) media, was added to each well and cells were incubated for 4 h at 37°C and kept in the dark. The MTT solution was then discarded and 100 µL of dimethyl sulfoxide was added into each well to dissolve insoluble formazan crystals and was incubated for 5 min. The optical density (OD) was measured at a test wavelength of 492 nm using a Shimadzu Multiwell plate reader. The OD values are used to calculate the percentage of proliferation using the formula below:

$$\text{Proliferation} = \frac{\text{OD}_{\text{test}} - \text{OD}_{\text{blank}}}{\text{OD}_{\text{control}} - \text{OD}_{\text{blank}}} \times 100.$$

ACKNOWLEDGEMENTS

The authors are thankful to the Institute of Excellence, Vijnana Bhavana, University of Mysore for providing spectral data.

FUNDING

The single crystal XRD studies were performed on a D8 Venture diffractometer funded by the NSF (MRI CHE1625732) and the University of Kentucky.

CONFLICT OF INTEREST

The authors declare no conflict of interest.

SUPPLEMENTARY INFORMATION

The online version contains supplementary material available at <https://doi.org/10.1134/S1070363224080267>.

REFERENCES

- Jarbrink, K., Ni, G., Sönnergren, H., Schmidtchen, A., Pang, C., Bajpai, and Josip, R., *Syst. Rev.*, 2017, vol. 6, p. 15.
<https://doi.org/10.1186/s13643-016-0400-8>
- Boakye, Y.D., Agyare, C., Ayande, G.P., Titiloye, N., Asiamah, E.A., and Danquah, K.O., *Front. Pharmacol.*, 2018, vol. 9, p. 945.
<https://doi.org/10.3389/fphar.2018.00945>
- Singer, A.J. and Clark, R.A., *New Engl. J. Med.*, 1999, vol. 341, p. 738.
<https://doi.org/10.1056/NEJM199909023411006>
- Zahid, M., Lodhi, M., Rehan, Z.A., Tayyab, H., Javed, T., Shabbir, R., Mukhtar, A., El Sabagh, A., Adamski, R., and Sakran, M.I., *Molecules.*, 2021, vol. 26, p. 3284.
<https://doi.org/10.3390/molecules26113284>
- Zahid, M., Lodhi, M., Afzal, A., Rehan, Z. A., Mehmood, M., Javed, T., Shabbir, R., Siuta, D., Althobaiti, F., and Dessok, E.S., *Gels*, 2021, vol. 7, p. 107.
<https://doi.org/10.3390/gels7030107>
- Ahmad Shah, S.S., Rivera, G., Ashfaq, M., *Mini-Rev. Med. Chem.*, 2013, vol. 13, p. 70.
<https://doi.org/10.2174/138955713804484749>
- Casini, A., Scozzafava, A., and Supuran, C.T., *Curr. Med. Chem.*, 2002, vol. 9, p. 1167.
<https://doi.org/10.2174/0929867023370077>
- Al-Mohammed, N.N., Alias, Y., Abdullah, Z., Shakir, R.M., Taha, E.M., and Hamid, A.A., *Molecules*, 2013, vol. 18, p. 11978.
<https://doi.org/10.3390/molecules181011978>
- Aben, O. and Jhimli, B., *Biophys. Rev.*, 2021, vol. 13, p. 259.
<https://doi.org/10.1007/s12551-021-00795-9>
- Gorantla, V., Gundlac, R., Jadavc, S.S., Anugu, S.R., Chimakurthy, J., Nidasanametla, S.K., and Korupolu, R., *New J. Chem.*, 2017, vol. 41, p. 13516.
<https://doi.org/10.1039/C7NJ03332J>
- Abdel-Aziz, A.A.M., Angeli, A., El-Azab, A.S., Hammouda, M.E.A., El-Sherbeny, M.A., and Supuran, C.T., *Bioorg. Chem.*, 2019, vol. 84, p. 260.
<https://doi.org/10.1016/j.bioorg.2018.11.033>
- Capasso, C., and Supuran, C.T., *J. Enzym Inhib. Med. Chem.*, 2015, vol. 30, p. 325.
<https://doi.org/10.3109/14756366.2014.910202>

13. Isik, K. and Kocak, O.F., *Microbiol. Res.*, 2009, vol. 164, p. 49.
<https://doi.org/10.1016/j.micres.2006.11.002>
14. Chohan, Z.H., Rauf, A., Naseer, M.M., Somra, M.A., and Supuran, C.T., *J. Enzyme Inhib. Med. Chem.*, 2006, vol. 21, p. 173–177.
<https://doi.org/10.1080/14756360500533059>
15. Chibale, K., Haupt, H., Kendrick, H., Yardley, V., Saravanamuthu, A., Fairlamb, A.H., and Croft, S.L., *Bioorg. Med. Chem. Lett.*, 2001, vol. 11, p. 2655.
[https://doi.org/10.1016/S0960-894X\(01\)00528-5](https://doi.org/10.1016/S0960-894X(01)00528-5)
16. Supuran, C.T. and Casini, A., *Med. Res. Rev.*, 2003, vol. 23, p. 535.
<https://doi.org/10.1002/med.10047>
17. Andrews, K.T., Fisher, G.M., Sumanadasa, S.D.M., Adams, T.S., Moeker, J., Lopez, M., and Poulsen, A., *Bioorg. Med. Chem. Lett.*, 2013, vol. 23, p. 6114.
<https://doi.org/10.1016/j.bmcl.2013.09.015>
18. Puccetti, L., Fasolis, G., Vullo, D., Chohan, Z.H., Scozzafava, A., and Supuran, C.T., *Bioorg. Med. Chem. Lett.*, 2005, vol. 15, p. 3096.
<https://doi.org/10.1016/j.bmcl.2005.04.055>
19. Supuran, C.T., *Metabolites*, 2017, vol. 7, p. 48.
<https://doi.org/10.3390/metabo7030048>
20. Abbate, F., Winum, J.Y., Potter, B. V., Casini, A., Montero, L.-J., Scozzafava, A., and Supuran, C.T., *Bioorg. Med. Chem. Lett.*, 2004, vol. 14, p. 231.
<https://doi.org/10.1016/j.bmcl.2003.09.064>
21. Neri, D. and Supuran, C.T., *Nat. Rev. Drug Discov.*, 2011, vol. 10, p. 767.
<https://doi.org/10.1038/nrd3554>
22. Masini, E., Carta, F., Scozzafava, A., and Supuran, C.T., *Expert Opin. Ther. Pat.*, 2013, vol. 23, p. 705.
<https://doi.org/10.1517/13543776.2013.794788>
23. Monti, S.M. and Supuran, C.T., *Expert Opin. Ther. Pat.*, 2013, vol. 23, p. 737.
<https://doi.org/10.1517/13543776.2013.798648>
24. Supuran, C.T., *J. Enzym. Inhib. Med. Chem.*, 2012, vol. 27, p. 759.
<https://doi.org/10.3109/14756366.2012.672983>
25. Ovung, A. and Bhattacharyya, J., *Biophys Rev.*, 2021, vol. 13, p. 259.
<https://doi.org/10.1007/s12551-021-00795-9>
26. Masereel, B., Thiry, A., Dogne, J.M., and Supuran, C.T., *Curr. Pharm. Des.*, 2008, vol. 14, p. 661.
<https://doi.org/10.2174/138161208783877956>
27. Scozzafava, A., Supuran, C.T., and Carta, F., *Expert Opin. Ther. Pat.*, 2013, vol. 23, p. 725.
<https://doi.org/10.1517/13543776.2013.790957>
28. Supuran, C.T., *J. Enzym. Inhib. Med. Chem.*, 2016, vol. 31, p. 345.
<https://doi.org/10.3109/14756366.2015.1122001>
29. Carta, F., and Supuran, C.T., *Expert Opin. Ther. Pat.*, 2013, vol. 23, p. 681.
<https://doi.org/10.1517/13543776.2013.780598>
30. Boyd, A.E., *Diabetes*, 1988, vol. 37, p. 847.
<https://doi.org/10.2337/diab.37.7.847>
31. Carta, F., Mannelli, L.D.C., Pinard, M., Ghelardini, C., Scozzafava, A., McKenna, R., and Supuran, C.T., *Bioorg. Med. Chem.*, 2015, vol. 23, p. 1828.
<https://doi.org/10.1016/j.bmc.2015.02.027>
32. Shaw, W., Chang, C.Y., and Hsuet, M.Y., *Eur. J. Med. Chem.*, 2010, vol. 45, p. 2860.
<https://doi.org/10.1016/j.ejmech.2010.03.008>
33. Wang, L., Wang, T., Yang, B., Chen, Z., and Yang, H., *Med. Chem. Res.*, 2012, vol. 21, p. 124.
<https://doi.org/10.1007/s00044-010-9512-1>
34. Henderson, B.J., Carper, D.J., and Cestari, T.F.G., *J. Med. Chem.*, 2011, vol. 54, p. 8681.
<https://doi.org/10.1021/jm201294r>
35. Prime, M.E., Andersen, O.A., and Barker, J.J., *J. Med. Chem.*, 2012, vol. 55, p. 1021.
<https://doi.org/10.1021/jm201310y>
36. Rao, B.R., Katiki, M.R., and Dileep, K., *Lett. Org. Chem.*, 2019, vol. 16, p. 723.
<https://doi.org/10.2174/1570178615666181113094539>
37. Winthrop, E.L., Eobert, N.L., and Merle, E.A., *J. Pharm. Sci.*, 1962, vol. 51, p. 32.
<https://doi.org/10.1002/jps.2600510104>
38. Vijayashree, R.J., and Sivapathasundharam, B., *J. Oral Maxillofac Pathol.*, 2022, vol. 26, p. 6.
https://doi.org/10.4103/jomfp.jomfp_48_22
39. Lee, H.G. and Eun, H.C., *J. Dermatol. Sci.*, 1999, vol. 21, p. 176.
[https://doi.org/10.1016/S0923-1811\(99\)00037-7](https://doi.org/10.1016/S0923-1811(99)00037-7)
40. Etter, M.C., MacDonald, J.C., Bernstein, J., *Acta Crystallogr. (B)*, 1990, vol. 46, p. 256.
<https://doi.org/10.1107/S0108768189012929>
41. Sheldrick, G.M., *Acta Crystallogr. (A)*, 2015, vol. 71, p. 3.
<https://doi.org/10.1107/S2053229614024218>
42. Sheldrick, G.M., *Acta Crystallogr. (C)*, 2015, vol. 71, p. 3.
<https://doi.org/10.1107/S2053229614024218>
43. Spackman, P.R., Turner, M. J., McKinnon, J.J., Wolff, S.K., Grimwood, D.J., and Jayatilaka, D., *J. Appl. Cryst.*, 2021, vol. 54, p. 1006.
<https://doi.org/10.1107/S1600576721002910>
44. Parkin, S., *Acta Crystallogr. (E)*, 2021, vol. 77, p. 452.
<https://doi.org/10.1107/S205698902100342X>
45. Groom, C.R., Bruno, I.J., Lightfoot, M.P., and Ward, S.C., *Acta Crystallogr. (B)*, 2016, vol. 72, p. 171.
<https://doi.org/10.1107/S2052520616003954>
46. Mosmann, T., *J. Immunol. Methods*, 1983, vol. 65, p. 55.
[https://doi.org/10.1016/0022-1759\(83\)90303-4](https://doi.org/10.1016/0022-1759(83)90303-4)

Publisher's Note. Pleiades Publishing remains neutral with regard to jurisdictional claims in published maps and institutional affiliations.
AI tools may have been used in the translation or editing of this article.